Detailed Simulation of Offshore Wind Turbine

V.Leble*, G.N.Barakos†
University of Liverpool, School of Engineering, Harrison Hughes Building, Liverpool, L69 3GH, U.K.,
www.liv.ac.uk/engdept

1 Introduction

Wind is a substantial renewable energy source, and historical trends show the large development of on-shore wind turbine size and power capacity over last three decades. However, high potential sites on land are already occupied, and others are hard to utilise due to e.g. difficult access, high altitude, costly transportation and on-site assembly. Therefore, a recent trend is to exploit the off-shore wind potential and take advantage of the available space and steady winds. Shallow water regions suitable for constructing seabed-fixed off-shore wind turbines are also limited, and for sea depths exceeding 30-60 m, floating structures are become more economic. Hence, emphasis is placed on the development of floating offshore wind turbines (FOWTs). Unlike onshore machines, the FOWT is a highly dynamic system since it is simultaneously subjected to the wind and wave loads and only constrained by the mooring system. Further, the rotor frequency is low due to the large size of the blades, and wave frequencies may come close or coincide with the rotational frequency of the rotor. Therefore, it is important to develop a method for the analysis of this air-structure-water system. The purpose of this paper is to present such an algorithm and obtained demonstration results. For this, the Helicopter Multi-Block (HMB2) solver developed at Liverpool University[2] is used to solve for the aerodynamic forces acting on the wind turbine (WT) blades. Hydrodynamic forces on the support platform are solved using the Smoothed Particle Hydrodynamics (SPH) method.[4,14] Both solvers are coupled by exchanging information while the FOWT is represented by a lumped mass model.

2 Numerical methods

The HMB2 code is a 3D multi-block structured solver and solves the Navier-Stokes equations in the 3D Cartesian frame of reference. HMB2 solves the Navier-Stokes equations in integral form using the arbitrary Lagrangian-Eulerian formulation for time-dependent domains with moving boundaries. The solver uses a cell-centred finite volume approach combined with an implicit dual-time method.[8] The HMB2 solver has a library of turbulence closures including several one- and two- equation turbulence models, and turbulence simulation is also possible using either the Large-Eddy or the Detached-Eddy simulation approach.

The sea is modelled with the SPH method. Each SPH particle represents the volume of the fluid and moves according to the Navier-Stokes equations solved in the Lagrangian form. SPH offers a variety of advantages for fluid modelling, particularly those with a free surface and moving bodies. Due to the Lagrangian nature of the SPH method, the free surface requires no special treatment. Further, submerged bodies can be represented with particles. Therefore, it is natural for the method to include floating objects.

The motion of the FOWT components is computed with a multi-body model (MBDM) of rigid bodies and frictionless joints. Mooring cables are modelled as a set of springs and dampers, according to Savenije.[13] The coordinate partitioning method[7,12] is used to solve the resulting system of mixed differential-algebraic equations. The time integration scheme is explicit and can be either the Runge-Kutta method of fourth order or Euler's method. The non-linear position equations are solved using Newton-Raphson method with exact analytical Jacobian.

All solvers were validated separately before coupling. The HMB2 CFD solver has so far been validated for several wind turbine cases, including the NREL Annex XX experiments,[5] and the pressure and PIV data of the MEXICO project.[3] The SPH method was validated against the experiments of Greenhow and Lin[6] for the high speed entry of a half-buoyant solid cylinder into calm water. The MBDM was validated using simple mechanical systems of known solution[7] like 2D and 3D slider-crank mechanisms.

In the present work, the communication between the MBDM, SPH and HMB2 was established through the Message Passing Interface (MPI). Due to the Lagrangian nature of the SPH method, the submerged bodies can be represented with particles and do not require specific coupling. Therefore, by utilising MPI, the MBDM substituted the body motion routines of the SPH solver and reduced the number of coupled codes to two - SPH and HMB2. This implies that MBDM is advancing in time with the same integration scheme as SPH using a symplectic method in this case.[10]

*Presenting Author, vleble@liverpool.ac.uk
†Corresponding Author, g.barakos@liverpool.ac.uk

2.1 Coupling algorithm

Different coupling methods have been extensively studied during the past two decades. The multi-physics problem with adjacent domains can be simulated in a monolithic or in a partitioned way. The former refers to the flow equations and structural equations being solved simultaneously, while the latter means that they are solved separately. Considering that two validated solvers (HMB2 and SPH) are available, the emphasis is placed on partitioned algorithms.

The partitioned coupling can be weak or strong. If the coupling scheme does not involve Jacobians relating the solutions of the two solvers, the scheme is called weak or loose. Explicit coupling schemes, as the one used in this work, are weak. On the other hand, if a Jacobian is employed, the scheme is called strong or tight, as the solution is equivalent to what would be achieved by a monolithical formulation.[11]

In the present paper, a weakly coupled approach is employed. Both solvers are advancing with different but constant time steps. SPH employs time step of $\Delta t_{SPH} = 2 \cdot 10^{-4} s$, whereas HMB2 employs time step of $\Delta t_{HMB2} = 2 \cdot 10^{-2} s = 100 \Delta t_{SPH}$. The small time step for the SPH method is required by the explicit integration scheme. The HMB2 solver employs an implicit dual-time method[8] that is superior for larger time steps. Synchronisation of the solvers is performed at the end of each HMB2 step.

At the beginning of each synchronisation time step, the position and velocities of the rotor are transferred to the HMB2 aerodynamic solver, and forces and moments on the rotor are passed to the SPH. The two solvers are then advancing to a new time level with different methods and different number of steps. SPH performs 100 symplectic steps, while HMB2 performs 350 implicit pseudo-time steps. During the symplectic steps of the SPH code, the aerodynamic loads are kept constant (frozen). In return, the position and velocities of the rotor are kept constant during the implicit steps of HMB2. Once the synchronisation point is reached, the new position and velocities of all bodies, and rotor loads are obtained. Then, the algorithm proceeds to the new time level and information between the solvers is exchanged.

3 Test case description

A 10-MW wind turbine design[1] is used in this work. The rotor diameter is $178.3m$, and the wind turbine operates at a wind speed of $11m/s$ with a rotational speed of $8.824rpm$. The wind turbine is attached to the floating support which consists of three cylindrical floats that increase the buoyancy and stability of the structure. A schematic of the studied FOWT is shown in Figure 1.

In the present model, the FOWT is represented by three mooring lines and two bodies. The first body represents the rotor (three blades with the spinner), and the second body represents the combined nacelle, tower and floating support rigidly linked to each other. The two bodies are connected by a revolute joint and a constraint of constant rotational speed is applied to the rotor. The resulting system has 6 unconstrained degrees of freedom. The mechanical properties of the bodies and mooring lines are presented in Table 1.

The FOWT is placed in a shallow tank presented in Figure 1. The waves are generated using a paddle on one side, and dissipated using a beach-like slope on the other side of the tank. Waves are generated to represent the specific sea state corresponding to a given wind speed. Based on the measurements of annual sea state occurrences in the North Atlantic and North Pacific,[9] the wind speed of $11m/s$ corresponds to a sea state 4 with a mean wave height of $1.88m$ and a period of $8.8s$.

The aerodynamic grid consists of the rotor and nacelle *i.e.* the tower is not included (for economies in CPU time) and the effect of the blade passing on the tower is not investigated. The grid consists of $8mln$ cells, and the distribution of the grid nodes in vicinity to the blade surface is presented in Figure 2. The hydrodynamic domain is resolved using $5mln$ particles with initial uniform spacing of $0.625m$. Each of the solvers was executed separately before coupling to obtain a periodic solution of the loads. Once the initial conditions were obtained, the coupled computation was initiated.

4 Results

Results of the coupled computation are presented in Figure 3. The thrust of the rotor as function of time is shown in Figure 4(a). As can be seen, the FOWT moves in the direction of the thrust by about $0.25m$ (displacement in x), and sinks in water with a dynamic maximum of about $1m$ (displacement in z). The pitching motion is a result of combined action of thrust and waves, and maximum dynamic pitch is $0.12rad$ or 6.9 degrees (rotation about y axis). As wind turbine pitches under the the thrust force, the rotor moves in the direction of the wind (velocity in x direction in Figure 4(b)). In return, the thrust force decreases due to the smaller inflow speed and the orientation of the rotor disk. The inverse relation between the thrust force and x velocity of the hub is clear in Figure 4. The initial motion of the FOWT is dominated by the disbalance of the forces due to applied thrust, and the effect of the first wave passage is not visible. However, as a second wave approaches the support, additional positive moment about y axis is created, and is clearly visible in Figure 3(f). Figure 5 presents different position of the FOWT during the computation.

5 Conclusions

The paper presented a coupling method for the analysis of off-shore wind turbines. The HMB2 CFD solver was used for the analysis of blade aerodynamics and via a multi-body dynamics method it was coupled to a smoothed particle hydrodynamics tool to model the floating part of the turbine. The results showed that the weak coupling method put forward in this paper is adequate for the solution of the problem at hand. The work suffers from the lack of experimental data for a coupled system and for this reason validation was only possible for the components of the model.

Acknowledgments

The financial support of the Marie Curie Host Fellowships Program: FP7-PEOPLE-2012-ITN-309395 - New Materials And Reliability In Offshore Wind Turbines Technology "MARE-WINT" are gratefully acknowledged.

References

[1] C. Bak, F. Zhale, R. Bitsche, T. Kim, A. Yde, L. C. Henriksen, P. B. Andersen, A. Natarajan, and H. M.H. Description of the dtu 10 mw reference wind turbin. Technical Report I-0092, DTU Wind Energy, 2013.

[2] G. Barakos, R. Steijl, K. Badcock, and A. Brocklehurst. Development of cfd capability for full helicopter engineering analysis. In *31st European Rotorcraft Forum*, 2005. Paper No. 91.

[3] M. Carrión, R. Steijl, M. Woodgate, G. Barakos, X. Munduate, and S. Gomez-Iradi. Computational fluid dynamics analysis of the wake behind the mexico rotor in axial flow conditions. *Wind Energy*, 2014.

[4] M. Gomez-Gesteira, B. D. Rogers, A. J. C. Crespo, R. A. Dalrymple, M. Narayanaswamy, and J. M. Dominguez. Sphysics - development of a free-surface fluid solver - part 1: Theory and formulations. *Computers & Geosciences*, 48:289–299, Nov. 2012.

[5] S. Gómez-Iradi, R. Steijl, and G. N. Barakos. Development and validation of a cfd technique for the aerodynamic analysis of hawt. *Journal of Solar Energy Engineering*, 131(3):031009, 2009.

[6] M. Greenhow and W. M. Lin. Nonlinear-free surface effects: Experiments and theory. Technical Report 83-19, MIT, Dept. of Ocean Engineering, Sept. 1983.

[7] E. J. Haug. *Computer Aided Kinematics and Dynamics of Mechanical Systems. Vol. 1: Basic Methods.* Allyn & Bacon, Inc., Needham Heights, MA, USA, 1989.

[8] A. Jameson. Time dependent calculations using multigrid, with applications to unsteady flows past airfoils and wings. In *10th Computational Fluid Dynamics Conference*. American Institute of Aeronautics and Astronautics, 1991.

[9] W. T. Lee, S. L. Bales, and S. E. Sowby. *Standardized Wind and Wave Environments for North Pacific Ocean Areas.* David W. Taylor Naval Ship Research and Development Center, 1985.

[10] B. J. Leimkuhler, S. Reich, and R. D. Skeel. Integration methods for molecular dynamics. In *In Mathematical Approaches To Biomolecular Structure And Dynamics, IMA Volumes In Mathematics And Its Applications*, pages 161–185. Springer, 1996.

[11] H. G. Matthies, R. Niekamp, and J. Steindorf. Algorithms for strong coupling procedures. *Computer Methods in Applied Mechanics and Engineering*, 195(1718):2028 – 2049, 2006.

[12] P. E. Nikravesh. *Computer-aided Analysis of Mechanical Systems.* Prentice-Hall, Inc., Upper Saddle River, NJ, USA, 1988.

[13] L. B. Savenije, T. Ashuri, G. J. W. Bussel, and J. W. Staerdahl. Dynamic modeling of a spar-type floating offshore wind turbine. In *Scientific Proceedings European Wind Energy Conference & Exhibition*, 2010.

[14] M. A. Woodgate, G. N. Barakos, N. Scrase, and T. Neville. Simulation of helicopter ditching using smoothed particle hydrodynamics. In *39th European Rotorcraft Forum*, September 2013.

Table 1: Mechanical properties of the employed bodies and mooring lines.

Rotor	
m $[kg]$	$227,962$
I $[kg \cdot m^2]$	$\begin{bmatrix} 1.56 \cdot 10^8 & 0 & 0 \\ 0 & 7.84 \cdot 10^7 & 0 \\ 0 & 0 & 7.84 \cdot 10^7 \end{bmatrix}$
Nacelle, support and tower	
m $[kg]$	$4,223,938$
I $[kg \cdot m^2]$	$\begin{bmatrix} 2.03 \cdot 10^{10} & 0 & 0 \\ 0 & 2.03 \cdot 10^{10} & 0 \\ 0 & 0 & 2.81 \cdot 10^9 \end{bmatrix}$
Mooring lines	
120.0	Angle between adjacent lines $[°]$
20.6	Depth of anchors below SWL $[m]$
7.0	Depth of fairleads below SWL $[m]$
116.73	Length of the relaxed line $[m]$
$400 \cdot 10^6$	Mooring line extensional stiffness $[N/m]$
$40,000$	Mooring line damping coefficient $[Ns/m]$

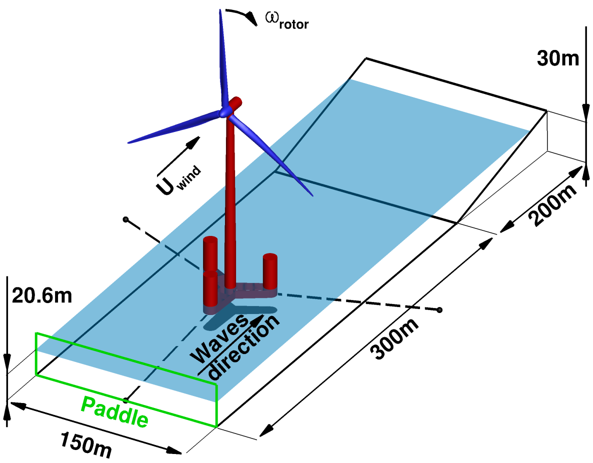

Figure 1: Schematic of the employed model of FOWT. Model consists of three mooring lines and two rigid bodies: the rotor (blue) and combined body representing nacelle, tower and support (red). Mooring lines are shown with dashed lines.

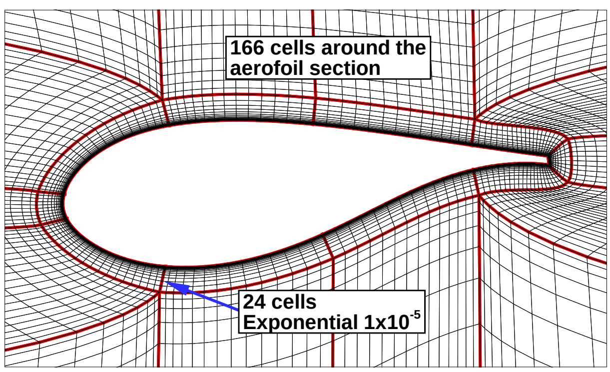

Figure 2: Slice through $8mln$ mesh used to solve for aerodynamic loads. View close to the blade surface.

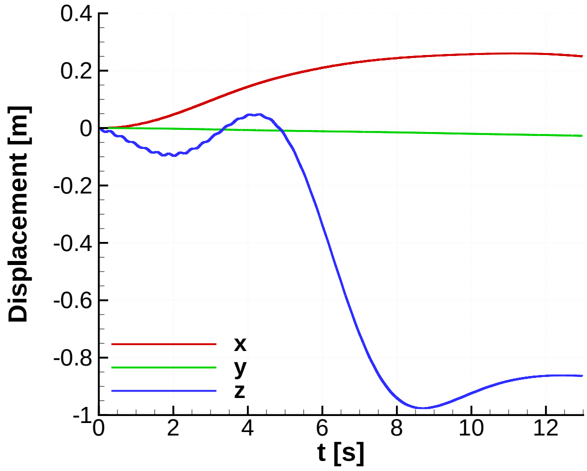

(a) Displacement of centre of gravity.

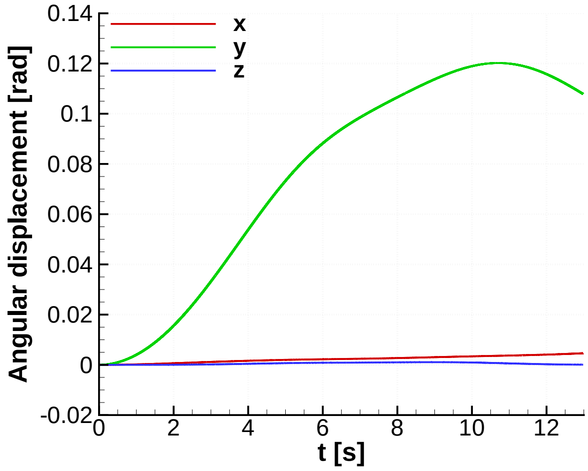

(b) Angular displacement.

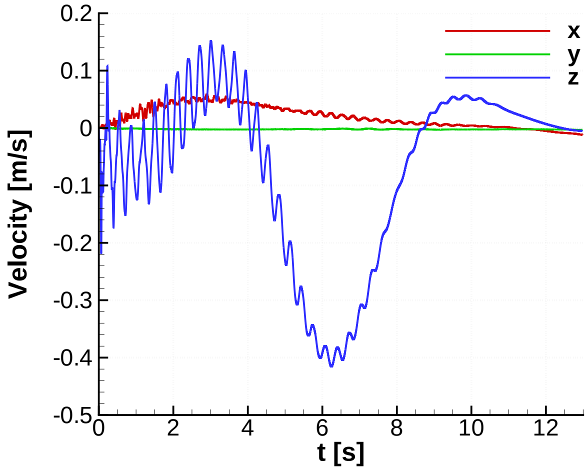

(c) Velocity of centre of gravity.

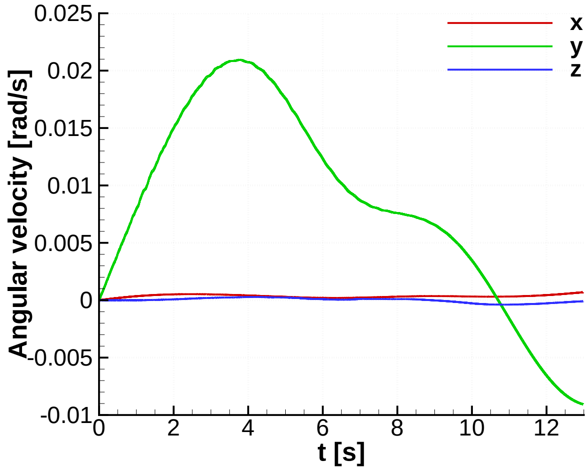

(d) Rotational velocity.

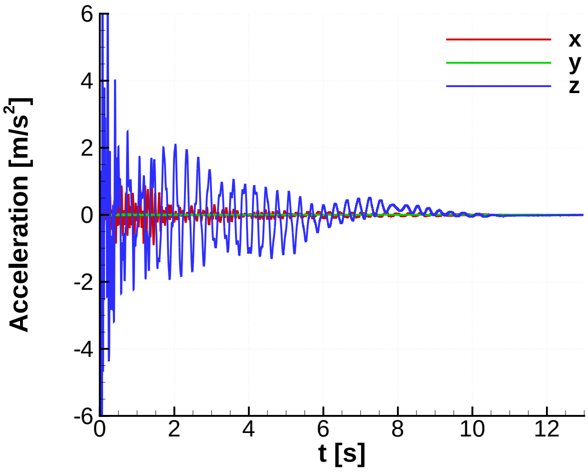

(e) Acceleration of centre of gravity.

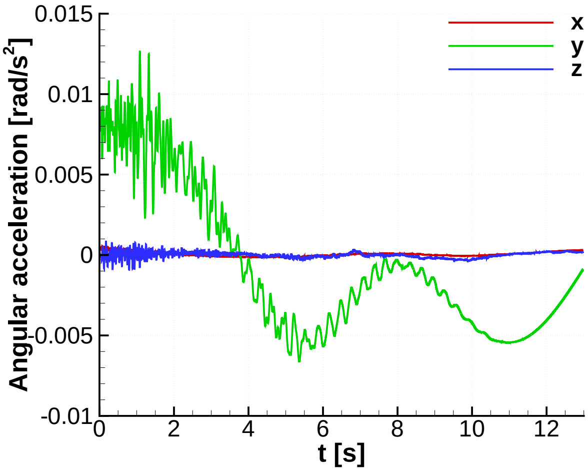

(f) Rotational acceleration.

Figure 3: Lateral and rotational dynamics of the support platform for coupled test case.

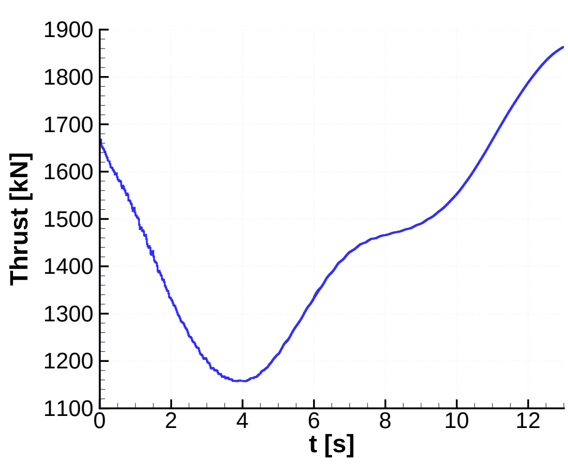

(a) Thrust of the rotor.

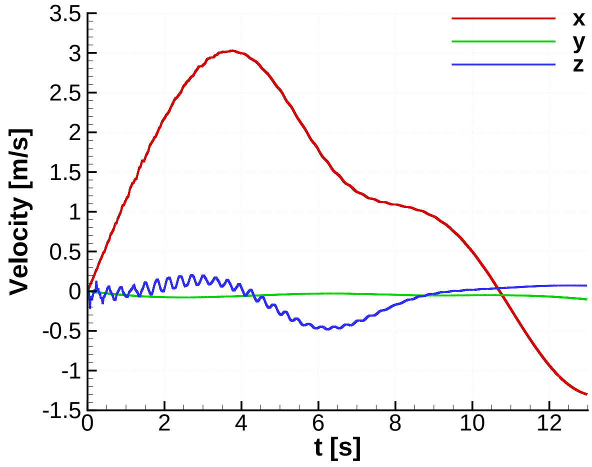

(b) Velocity of centre of gravity of the rotor.

Figure 4: Thrust of the rotor and velocity of centre of gravity of the rotor as function of time for coupled computation.

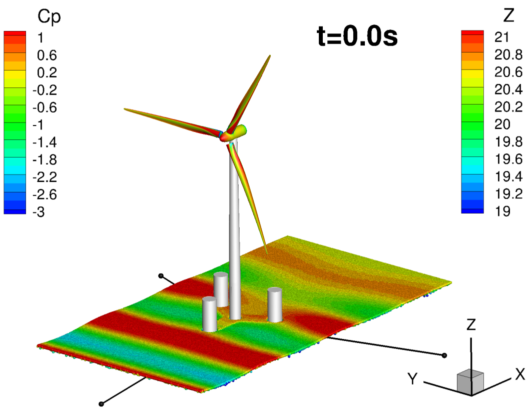

(a) Time $t = 0s$.

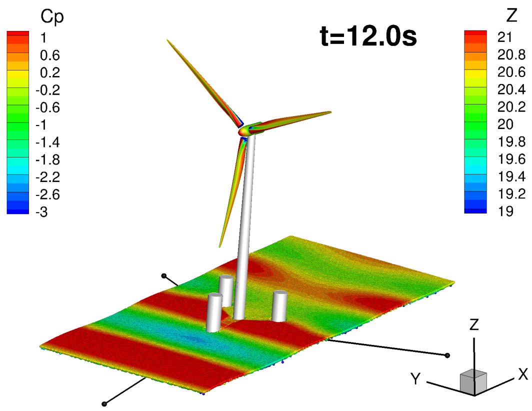

(b) Time $t = 12s$.

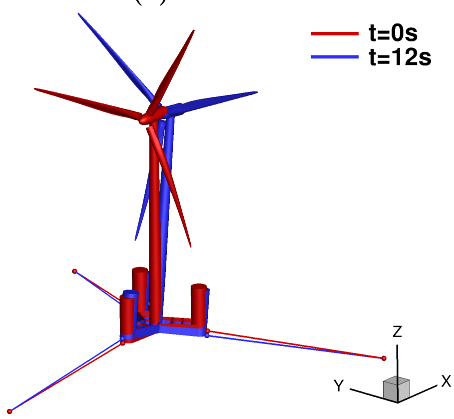

(c) Isometric view of position at times $t = 0s$ and $t = 12s$.

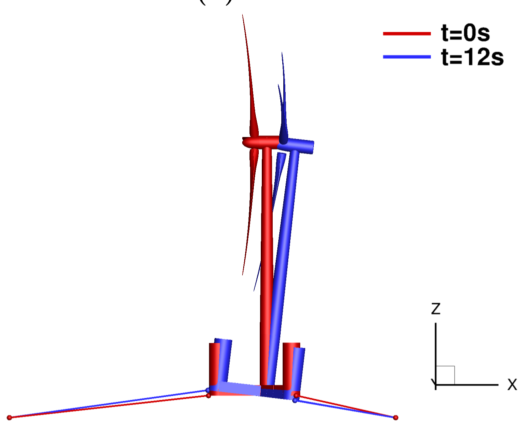

(d) Side view of position at times $t = 0s$ and $t = 12s$.

Figure 5: Position and orientation of the FOWT at times $t = 0s$ and $t = 12s$ during coupled computation. Contours on the rotor correspond to pressure coefficient Cp, contours on the water surface correspond to surface elevation z in meters.